Available online at www.sciencedirect.com
ScienceDirect
Trans. Nonferrous Met. Soc. China 27(2017) 420−428
Transactions of Nonferrous Metals Society of China
www.tnmsc.cn

Process optimization and kinetics for leaching of cerium, lanthanum and neodymium elements from iron ore waste's apatite by nitric acid

A. FERDOWSI, H. YOOZBASHIZADEH

Department of Materials Science and Engineering, Sharif University of Technology, Azadi Ave., Tehran, P. O. Box 11155-9466, Iran

Received 1 February 2016; accepted 4 July 2016

Abstract: The leaching of rare earth elements (REEs) including cerium, lanthanum and neodymium from apatite concentrate obtained from iron ore wastes by nitric acid was studied. The effects of nitric acid concentration, solid to liquid ratio and leaching time on the recoveries of Ce, La and Nd were investigated using response surface methodology. The results showed that the acid concentration and solid to liquid ratio have significant effect on the leaching recoveries while the time has a little effect. The maximum REE leaching recoveries of 66.1%, 56.8% and 51.7% for Ce, La and Nd, respectively were achieved at the optimum leaching condition with 18% nitric acid concentration, 0.06 solid to liquid ratio and 38 min leaching time. The kinetics of cerium leaching was investigated using shrinking core model. It was observed that the leaching is composed of two stages. In the first stage a sharp increase in cerium leaching recovery was observed and at the longer time the leaching became slower. It was found that in the first stage the diffusion of reactants from ash layer is the rate controlling mechanism with an apparent activation energy of 6.54 kJ/mol, while in the second stage the mass transfer in the solution is the controlling mechanism.
Key words: rare earth elements; apatite; leaching; response surface methodology; shrinking core model

1 Introduction

The demand for rare earth (RE) metals and their compounds are increasing rapidly due to their unique magnetic, electrical, chemical, catalytic, optical and spectroscopic properties that have led to their application in many fields of advanced materials applications [1−3]. They have applications in numerous fields including electronic, metallurgy, petroleum, textiles, and agriculture, and they are also becoming uniquely indispensable and critical in many high-tech industries such as hybrid cars, wind turbines, and compact fluorescent lights, flat screen televisions, mobile phones, disc drives, and defense technologies [3]. There are a wide variety of rare earth minerals, but notably the mined minerals are bastnasite, monazite, and xenotime [3−5]. Apatite, cheralite, eudialyte, loparite, and phosphorites make up the remaining resources [3]. Apatite containing average 0.1%−0.8% rare earth oxides is the main source of phosphate fertilizers and phosphoric acid. In spite of its low rare earth content apatite could become an important source of rare earths because it is processed in large quantities [6]. Different processes for extracting race earth elements (REEs) from apatite are investigated. Leaching with sulfuric acid is the most common method for treating apatite [5]. During the manufacture of phosphoric acid about 70% of rare earth element is lost in the gypsum. However, if leaching is conducted by nitric acid, most of the rare earths substituted in the apatite lattice for calcium ions will go into solution, and the rate of REEs recovery is essentially higher than that when using sulfuric acid [7,8]. Besides, nitrate solutions are more preferable for extraction and separation of the REEs [9]. Hydrochloric acid is also used for dissolution of apatite for extraction of rare earths [7], however, the application of this acid is very limited.

Leaching of apatite in different acid media has been extensively studied [10−16]. However, there are few works on the leaching behavior of REEs from apatite. GUMGUM [17] studied the effect of acid concentration, agitation time and solid to liquid ratio on the leaching of yttrium from apatite by sulfuric acid. KHAWASSEK et al [18] studied the effect of acid concentration, agitation time, ore particle size, acid to ore ratio, temperature and

Corresponding author: A. FERDOWSI; Tel: +98-21-6616-4685; E-mail: ferdowsi79@yahoo.com
DOI: 10.1016/S1003-6326(17)60048-7

addition of H_2O_2 as oxidant on sulfuric acid leaching of apatite. WANG et al [19] investigated the influence of phosphoric acid concentration, temperature, liquid to solid ratio and additives on the REEs leaching efficiencies in digestion of apatite by sulfuric acid. They reported that REEs leaching recoveries increased by decreasing temperature and increasing the concentration of phosphoric acid and liquid/solid ratio. KANDIL et al [20] investigated the effect of acid concentration, flow rate and the presence of additives on the column leaching of REEs from apatite by hydrochloric acid, nitric acid and sulfuric acid solutions. They studied the kinetics of leaching by shrinking core model and reported that the rate controlling step is diffusion through ash layer and the activation energy for leaching is calculated accordingly. JORJANI et al [21] studied the effect of acidity, pulp density, agitation rate and time on the leaching recoveries of REEs from apatite by nitric acid. They used laboratory data to predict mathematical models for recoveries of REEs as function of various factors.

In the present work, apatite was leached by nitric acid and the effects of main process parameters including acid concentration, solid to liquid ratio and leaching time were investigated. For this purpose, the response surface methodology (RSM) and experiment design were employed and the influence of parameters affecting the leaching process and optimum condition were obtained. The kinetics of REEs leaching from apatite was also investigated and the controlling kinetic model of the reaction process was determined.

2 Experimental

2.1 Materials and apparatus

The apatite sample was the product of processing plant of Chadormalu Iron Ore Mine of Iran. The particle size of apatite concentrate was below 50 μm and no further grinding was performed. Nitric acid of analytical grade (Merck) was applied as leaching agent. XRD experiments were carried out to determine the mineralogical analysis of apatite sample. The rare earth elements in the apatite were determined by ICP-MS and for leaching samples by ICP-AES.

2.2 Leaching experiments

Leaching tests were carried out in a 200 mL glass reactor on a magnetic heater and stirrer. It has been reported that temperature has no significant effect on REEs leaching recoveries from apatite but higher temperature has favor advantageous due to volatilization of flour and sulfur [22]. Therefore, all leaching tests for optimization were performed at 60−70 °C. The pulp was stirred at an agitation speed of 800 r/min by magnet stirrer in all tests including optimization and kinetics studies. Samples were taken after reaction period at pre-determined intervals and were filtered using a filter paper. The filtrate solution was analyzed for REEs and the leaching recovery was determined by the following equation:

$$R = \frac{C_L}{BC_A} \times 100\% \quad (1)$$

where R is the leaching recovery, B is the solid to liquid ratio, and C_L and C_A are the concentrations of REE in the leachate and apatite sample, respectively.

2.3 Design of experiments (DOE)

Response surface methodology (RSM) is widely used for optimization of process variable in many chemical systems. RSM helps to decrease the number of experiments needed for analyzing the process, and also analyze the interaction between the parameters [23]. Central composite design (CCD) was employed for experimental design. Nitric acid concentration, solid/liquid ratio and leaching time were chosen as the independent variables with their levels and ranges shown in Table 1. The chosen independent variables used in the process optimization were coded according to

$$X_i = \frac{x_i - x_0}{\Delta x} \quad (2)$$

where X_i is the dimensionless coded value of each independent variable, x_0 is the value of x_i at the center point and Δx is the step change value.

Table 1 Independent variables and their levels used in RSM design

Variable	Symbol	Range and level		
		−1	0	+1
Nitric acid concentration/%	*A*	10	20	30
Solid/liquid ratio	*B*	0.05	0.075	0.1
Leaching time/min	*C*	10	35	50

The leaching recoveries of lanthanum, cerium and neodymium were the response variables of the experimental conditions in the design of experiments. The nitric acid concentration was varied from 10% to 30%, the solid/liquid ratio was varied from 0.05 to 0.10, and the leaching time was selected in the range of 10 to 60 min. A total of 18 experiments consisting of 8 factorial points, 6 axial points and 4 replicates at the central points were carried out. The experimental results obtained from the CCD model were described by a second order polynomial as a function of X_i as given

$$Y = \beta_0 + \sum_{i=1}^{n} \beta_i X_i + \sum_{i=1}^{n} \beta_{ii} X_i^2 + \sum_{i<j}^{n} \beta_{ij} X_i X_j \quad (3)$$

where β_0 is the value for the fixed response at the central point of the experiment; and β_i, β_j and β_{ij} are the linear, quadratic and cross product coefficients, respectively. The analyses of variance (ANOVA) and response surfaces were performed using the Design-Expert software (version 7.0.0) from Stat-Ease Inc., USA. The optimized leaching conditions were estimated using the software's numerical and graphical optimization tools.

3 Results and discussion

3.1 Analysis

The assay of rare earth elements in apatite is presented in Table 2. It shows that lanthanum, cerium and neodymium comprise more than 77% of total rare earth elements of apatite.

Table 2 Assay of rare earth elements in apatite sample (10^{-6})

La	Ce	Pr	Nd	Sm	Eu	Gd
1551	3707	559.27	1832.2	277.48	26.37	219.66
Tb	Dy	Er	Tm	Yb	Lu	Y
28.3	136.8	62.81	7.1	40.1	4.49	655.5

The XRD analysis revealed that flourapatite, calcite, ankerite, hematite and quartz are the main minerals in apatite concentrate while flourapatite is the dominant one (Fig. 1).

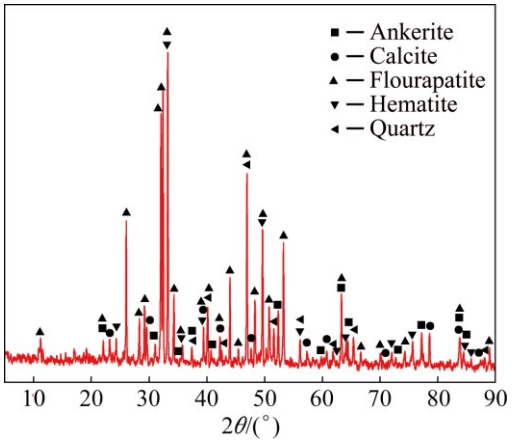

Fig. 1 XRD analysis of apatite sample

3.2 Response analysis and interpretation

Central composite design (CCD) was employed to develop correlation between the leaching process variables and the leaching recoveries. The complete design matrix together with the responses achieved from the experimental works is given in Table 3. The highest leaching recoveries were achieved for cerium while the lowest recoveries were for neodymium. In the experiments condition, the leaching recoveries for Ce, La and Nd were in the range of 12.64%−64.46% for cerium, 11.35%−56.11% for lanthanum and 10.84%−50.13% for neodymium.

Table 3 Experimental design matrix and results

Run	A/%	B	C/min	Recovery/%		
				Ce	La	Nd
1	20	0.075	35	62.27	52.44	48.72
2	10	0.05	60	60.31	52.15	47.41
3	30	0.05	10	62.98	54.15	49.76
4	20	0.075	35	58.88	48.89	47.88
5	10	0.1	60	20.11	17.55	17.01
6	20	0.075	35	59.55	53.68	47.36
7	30	0.1	60	59.51	50.23	45.83
8	10	0.075	35	43.33	36.36	34.03
9	20	0.075	35	60.52	51.47	46.76
10	20	0.05	35	64.29	55.58	50.13
11	10	0.1	10	12.64	11.35	10.84
12	10	0.05	10	57.27	49.12	44.91
13	20	0.075	60	62.86	52.84	48.76
14	30	0.1	10	54.51	46.47	41.91
15	20	0.075	10	59.40	50.09	45.69
16	20	0.1	35	48.26	40.77	36.58
17	30	0.075	35	63.58	53.98	49.23
18	30	0.05	60	64.46	56.11	50.10

To select the best model which could fit the experimental data, the sum of squares for polynomial models including mean, linear, 2FI, quadratic and cubic models were calculated by Design-Expert software. The models were selected based on the highest order polynomials where the additional model terms were significant and model was not aliased or meaningless. The quadratic models were suggested by software and were selected for leaching recoveries of each element. The adequacy of the models was further justified through analysis of variance (ANOVA). The ANOVA of quadratic models for leaching recoveries of Ce, La and Nd are presented in Tables 4, 5 and 6, respectively. From the ANOVA for response surface quadratic model for leaching recoveries, the model F-value of 84.09, 74.85 and 114.53 for Ce, La and Nd, respectively, imply that the models were meaningful. The values of Prob>F less than 0.05 indicate that the model term has significant effect on the response. Therefore, the effects of all model's parameters on leaching recoveries were not significant and for the leaching recoveries of Ce, La and Nd, nitric acid concentration (A), solid to liquid ratio (B), time (C) and AB, A^2, B^2 were significant model terms whereas the other terms were insignificant. In order to enhance the effect of significant parameters, the

Table 4 ANOVA for response surface quadratic model for Ce leaching recovery

Source	Sum of squares	df	Mean square	*F*-value	*P*-value Prob>*F*
Model	3708.402	9	412.0446	84.08865	< 0.0001
A	1240.6	1	1240.6	253.1773	< 0.0001
B	1305.911	1	1305.911	266.5059	< 0.0001
C	41.75592	1	41.75592	8.521405	0.0193
AB	637.6405	1	637.6405	130.1275	< 0.0001
AC	2.027562	1	2.027562	0.413778	0.5381
BC	7.905421	1	7.905421	1.613311	0.2397
A^2	145.8088	1	145.8088	29.75616	0.0006
B^2	55.23756	1	55.23756	11.27269	0.0100
C^2	0.311009	1	0.311009	0.06347	0.8074
Residual	39.20097	8	4.900122		

Table 5 ANOVA for response surface quadratic model for La leaching recovery

Source	Sum of squares	df	Mean square	*F*-value	*P*-value Prob>*F*
Model	2689.105	9	298.7895	74.85277	< 0.0001
A	891.3418	1	891.3418	223.299	< 0.0001
B	1014.87	1	1014.87	254.2453	< 0.0001
C	31.29524	1	31.29524	7.840087	0.0232
AB	432.4809	1	432.4809	108.3452	< 0.0001
AC	1.549775	1	1.549775	0.38825	0.5506
BC	3.102284	1	3.102284	0.777184	0.4037
A^2	105.3082	1	105.3082	26.38182	0.0009
B^2	28.19069	1	28.19069	7.062335	0.0289
C^2	0.010096	1	0.010096	0.002529	0.9611
Residual	31.93357	8	3.991696		

Table 6 ANOVA for response surface quadratic model for Nd leaching recovery

Source	Sum of squares	df	Mean square	*F*-value	*P*-value Prob>*F*
Model	2155.714	9	239.5238	114.5329	< 0.0001
A	682.7238	1	682.7238	326.4575	< 0.0001
B	812.3202	1	812.3202	388.4264	< 0.0001
C	25.60652	1	25.60652	12.24425	0.0081
AB	342.5228	1	342.5228	163.7838	< 0.0001
AC	2.440408	1	2.440408	1.166928	0.3115
BC	6.56334	1	6.56334	3.138386	0.1144
A^2	79.94931	1	79.94931	38.22929	0.0003
B^2	37.2709	1	37.2709	17.8218	0.0029
C^2	0.073037	1	0.073037	0.034924	0.8564
Residual	16.73048	8	2.09131		

insignificant parameters were eliminated from the quadratic models. The final equations in terms of coded factors for the leaching recoveries are shown as follows:

$$\text{Ce recovery} = 60.60+11.14A-11.43B+2.04C+8.93AB-7.22A^2-4.39B^2 \quad (4)$$

$$\text{La recovery} = 51.52+9.44A-10.07B+1.77C+7.35AB-6.21A^2-3.20B^2 \quad (5)$$

$$\text{Nd recovery} = 47.40+8.26A-9.01B+1.60C+6.54AB-5.37A^2-3.65B^2 \quad (6)$$

The validation of model was an important part of the data analysis procedure, since an inadequate model could lead to misleading results. “Adequate Precision” measures the signal to noise ratio. A ratio greater than 4 is desirable [24,25]. For fixed models the adequate precision ratios for leaching of Ce, La and Nd were 39.466, 39.495 and 41.673, respectively, which indicate an adequate signal and these models can be used to navigate the design space. The predicted leaching recoveries are compared with the actual leaching recoveries in Fig. 2. The correlation coefficients (R^2) for models were found to be 0.99 which are close to unity, indicating good agreement between the experimental and the predicted leaching recoveries.

3.3 Effect of variables on response and optimization

The influences of nitric acid concentration, solid to liquid ratio and leaching time on the leaching recoveries of Ce, La and Nd were evaluated. The results showed that the concentration of nitric acid has the most effect on the leaching recoveries while the leaching time has little influence on the REE recoveries. Figure 3 shows the effect of nitric acid concentration on the Ce, La and Nd leaching recovery. As it is illustrated in Fig. 3, the acid concentration and solid/liquid ratio have interaction on each other. At the low solid/liquid ratio (S/L=0.05), increasing the acid concentration has little effect on the Ce leaching recovery while at higher solid/liquid ratio (S/L=0.10) increasing acid concentration has a significant effect on the leaching recovery. This phenomenon is a result of the nature of leaching reaction of apatite by nitric acid.

$$Ca_{10}(PO_4)_6F_2+20HNO_3=10Ca(NO_3)_2+6H_3PO_4+2HF \quad (7)$$

REEs are substituted by calcium in apatite structure. On leaching of apatite, first all calcium was dissolved in the nitric acid [26] and therefore, for successive leaching of REEs the number of moles of nitric acid entering the system should be at least 20 times more than the number of moles of apatite which are subject to leaching. Furthermore, according to Reaction (7), phosphoric acid is generated during the leaching process, and due to the low solubility of RE phosphates (lg K_{sp} for La, Ce and Nd phosphates are too close and approximately equal to −26 [27]), the REEs leaching recoveries are restricted.

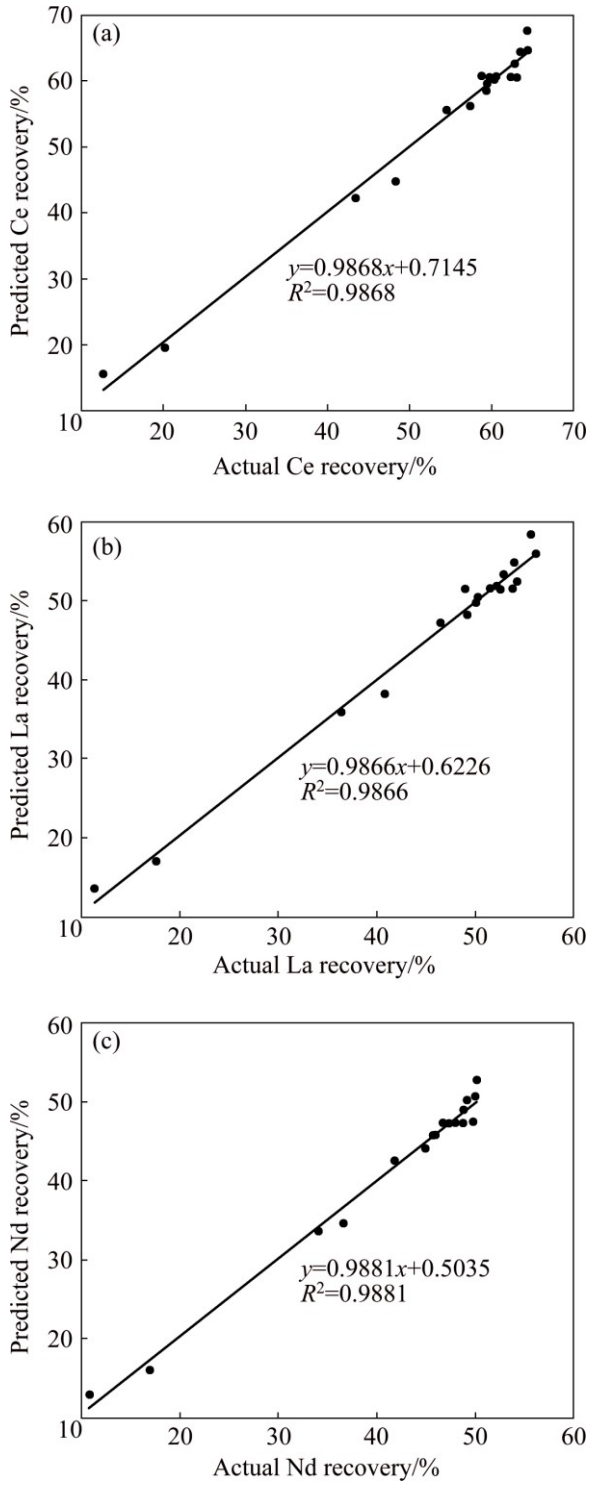

Fig. 2 Comparison of model prediction with experimental data for leaching of Ce (a), La (b) and Nd (c)

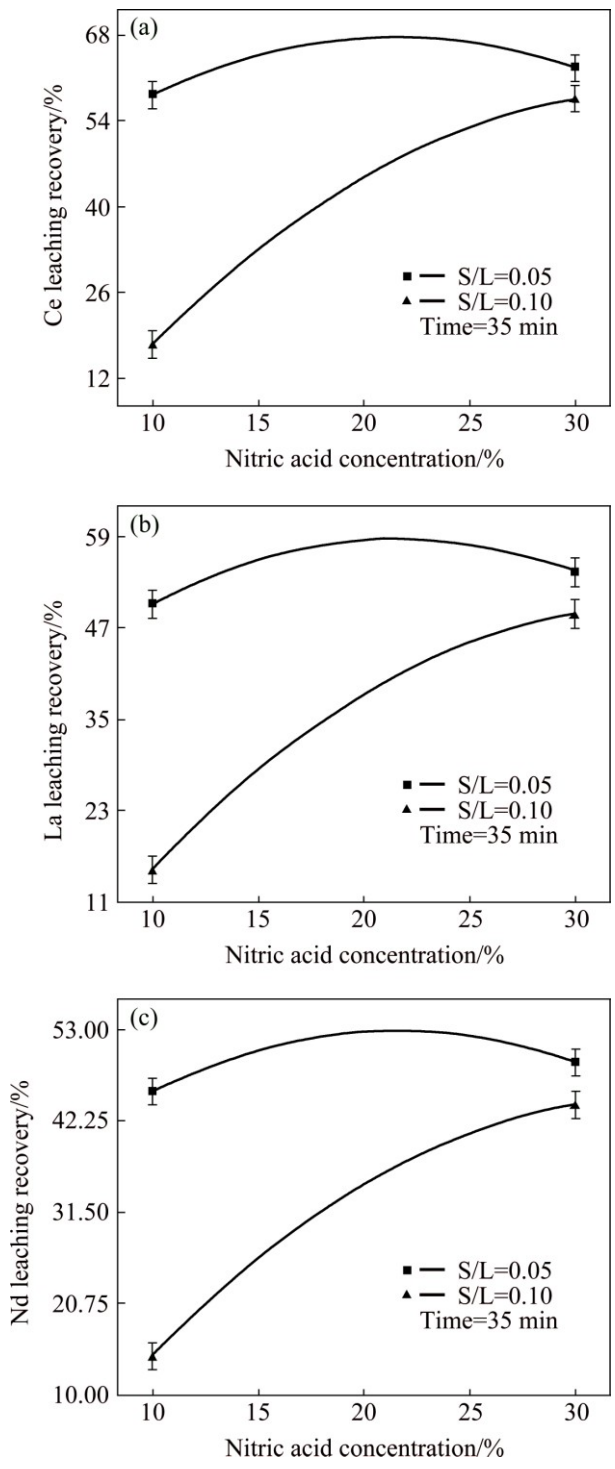

Fig. 3 Effect of nitric acid concentration on Ce (a), La (b) and Nd (c) leaching recoveries

The effect of leaching time on REEs leaching recoveries is shown in Fig. 4. The leaching time has no significant effect on the leaching recovery.

The three-dimensional response surfaces which show the effects of nitric acid concentration and solid/liquid ratio on the REE leaching recoveries are presented in Fig. 5.

3.4 Process optimization

With the objective of maximizing leaching recoveries at the lowest nitric acid concentration and leaching time and highest solid to liquid ratio, the optimum conditions were identified using the Design-Expert software. It reports the optimum condition to be a nitric acid concentration of 19%, solid to liquid ratio of 0.08 and leaching time of 10 min which results in the

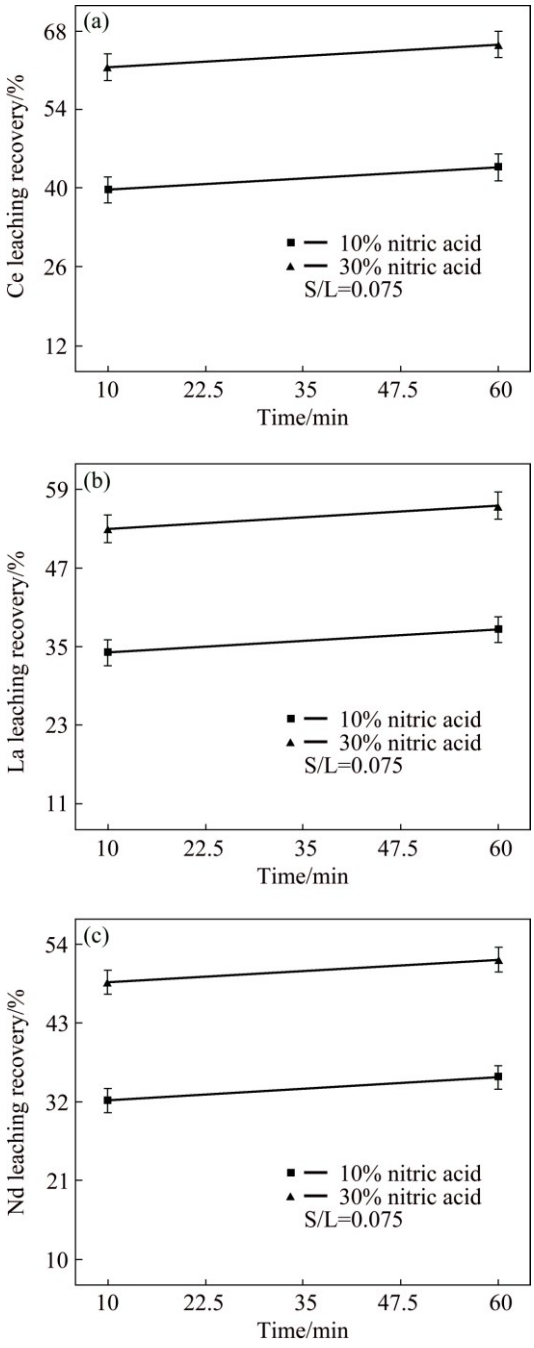

Fig. 4 Effect of leaching time on REEs leaching recovery

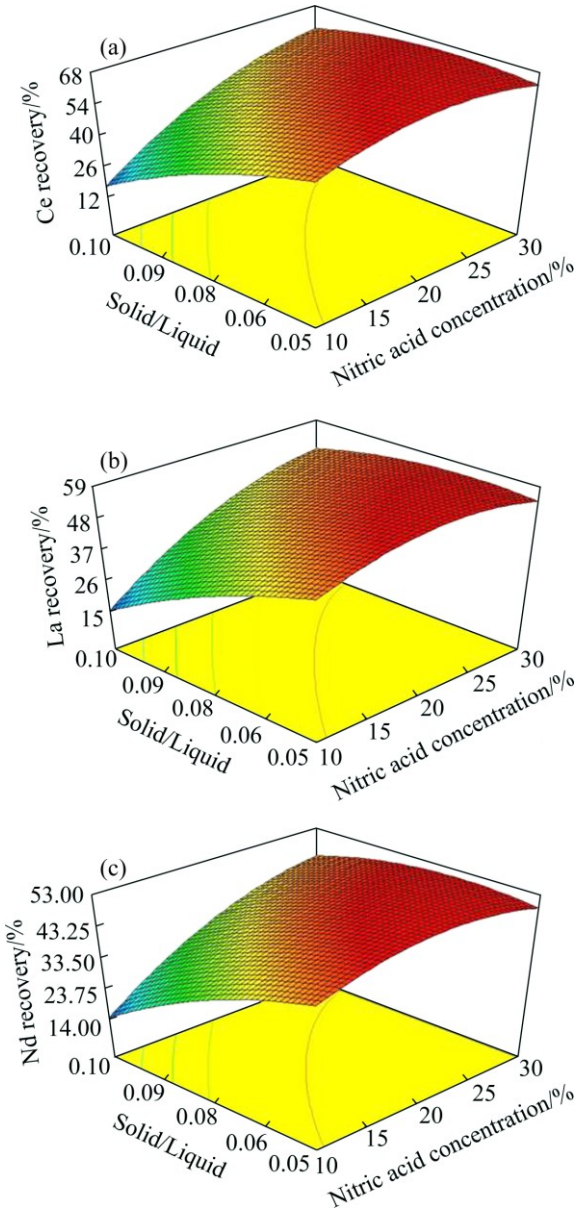

Fig. 5 Effect of nitric acid concentration and solid/liquid ratio on leaching recovery (leaching time: 35 min)

leaching recoveries of 56.3%, 47.8% and 44.1% for Ce, La and Nd, respectively. However, when no constrain was applied on the process parameters, for maximizing REE recoveries the optimum conditions were determined as 18%, 0.06 and 38 min for nitric acid concentration, solid/liquid ratio and time, respectively. At these conditions the leaching recoveries for Ce, La and Nd were 66.1%, 56.8% and 51.7%, respectively.

3.5 Kinetics study

Leaching experiments imply that at the studied conditions, Ce, La and Nd have similar behavior on leaching by nitric acid. On the other hand, Ce is the most available REE in the apatite and its leaching recovery is more than those of La and Nd. Therefore, kinetics studies were carried out on the Ce dissolution. The kinetics of Ce dissolution from apatite concentrate was analyzed using the data obtained with 10% (volume fraction) nitric acid at different temperatures and a solid to liquid ratio equal to 0.05. Figure 6 shows the effect of leaching temperature on the cerium recovery. The mechanism of leaching of REEs was examined by shrinking core model for spherical particle constant size [28]. Equations for film diffusion control (Eq. (8)), ash diffusion control (Eq. (9)), and reaction control (Eq. (10)) were examined on the leaching data.

$$kt=X \quad (8)$$

$$kt=1-3(1-X)^{2/3}+2(1-X) \quad (9)$$

$$kt=1-(1-X)^{1/3} \quad (10)$$

where k is the apparent reaction rate constant, t is the time and X is the leaching recovery.

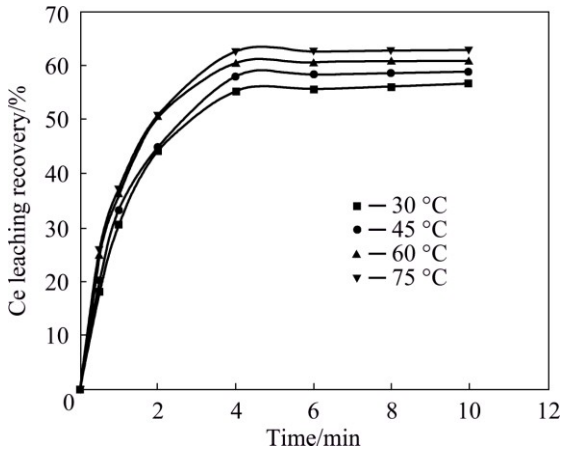

Fig. 6 Effect of temperature on Ce recovery (Nitric acid concentration: 10%; S/L: 0.05; agitation: 800 r/min)

From Fig. 6, it is clear that there are two different stages on the leaching of REEs. The rate of leaching at the first stage (before 4 min) is considerably different from that of the second stage (after 4 min). Beside when any of the equations related to different controlling mechanisms (Eqs. (8)−(10)) was examined with the experimental data for the whole leaching period, a significant change in the trend before and after 4 min was observed. This also indicates that the whole leaching period is not governed by a single mechanism. As a result, in the following discussion, the controlling mechanisms in the REEs leaching from apatite were examined for short time (less than 4 min) and long time (more than 4 min) stages, separately [29].

Data analysis showed that, at the studied conditions, chemical reaction control is not the governing mechanism for the leaching of rare earths from apatite with nitric acid.

It was found that at short time, data fit with ash diffusion control mechanism. Figure 7 shows a plot of $1-3(1-X)^{2/3}+2(1-X)$ versus time. This plot is close to a straight line with an acceptable correlation coefficient. The reaction rate constant for ash diffusion was determined from the slope of the lines.

Data analysis showed that at the second stage of the leaching process (after 4 min), the leaching recoveries fit the film diffusion control mechanism. It should be noted that the data for long time studies should be modified since at the beginning of second stage the time and leaching recovery were not zero. So the time at 4 min and the recoveries at this time were applied as zero for analyzing the second stage of leaching. Figure 8 shows a plot of leaching recovery versus time in which the time and Ce recovery were modified. The change in leaching mechanism at the long time process is a result of the consumption of reactant acid and decreasing the acid concentration in the solution. Therefore, transferring reactant to the surface of apatite is the reaction rate controlling at this condition.

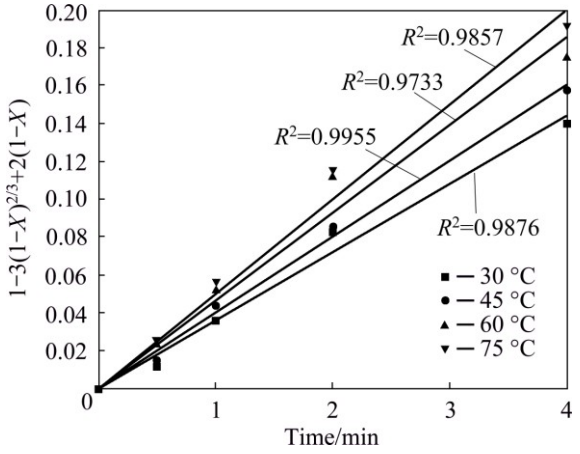

Fig. 7 Plot of $1-3(1-X)^{2/3}+2(1-X)$ vs time at different temperatures at short time

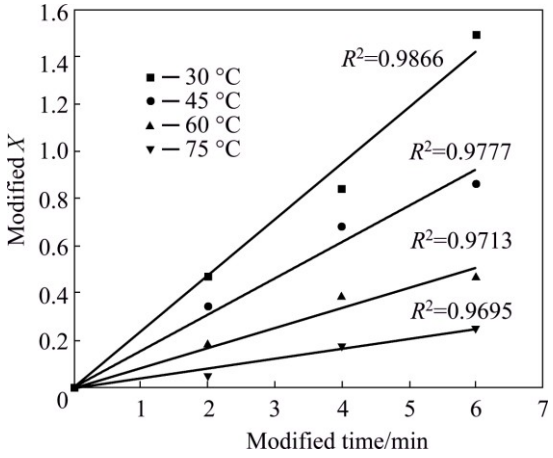

Fig. 8 Plot of modified time vs modified leaching recovery at different temperatures for long term process

The reaction rate constants for each stage of process were determined from the slope of the lines in Figs. 7 and 8. The activation energy for each step of reaction was determined by Arrhenius plots of ln k vs $1/T$ which are presented in Figs. 9 and 10. From the Arrhenius plots, the activation energies of 6.54 kJ/mol and −33.86 kJ/mol were calculated for the cerium dissolution at ash diffusion and film diffusion control, respectively.

4 Conclusions

The effect of nitric acid concentration, solid to liquid ratio and time on the leaching of rare earth

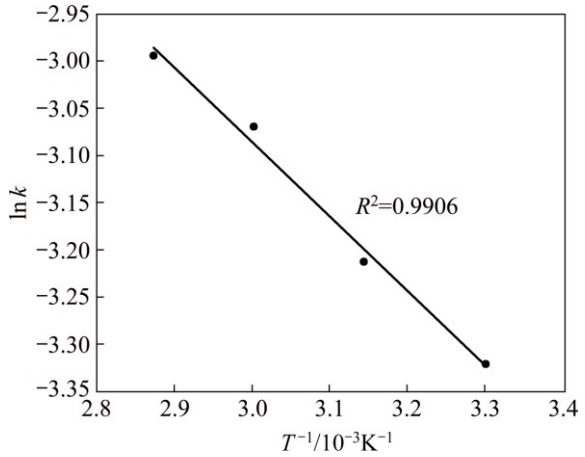

Fig. 9 Arrhenius plot for short time leaching of cerium from apatite by nitric acid

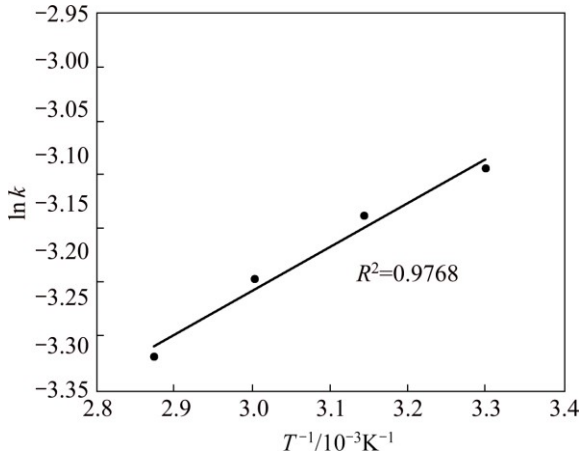

Fig. 10 Arrhenius plot for long time leaching of cerium from apatite by nitric acid

elements (Ce, La and Nd) from apatite concentrate was investigated using response surface methodology. The proposed quadratic models were conformed well to experimental data with correlation coefficients (R^2) of 0.98. It was found that the nitric acid concentration and solid/liquid ratio have significant effect on the REEs leaching recoveries, while leaching time has little effect. Using Design-Expert software, the optimum conditions were determined to be a nitric acid concentration of 18%, solid/liquid ratio of 0.06 and leaching time of 38 min, with leaching REEs recoveries of 66.1%, 56.8% and 51.7% for Ce, La and Nd, respectively.

The kinetics of leaching of cerium from apatite was examined using shrinking core model. Two different stages in the leaching of Ce from apatite by nitric acid were observed. In the first stage (shorter than 4 min) the diffusion of reactants from ash layer was the rate controlling step with an apparent activation energy of 6.54 kJ/mol, while in the second stage of leaching, the reactant transfer from liquid phase to surface of apatite is the controlling mechanism of Ce leaching.

References

[1] ALONSO E, SHERMAN A M, WALLINGTON T J, EVERSON M P, FIELD F R, ROTH R, KIRCHAIN R E. Evaluating rare earth element availability: A case with revolutionary demand from clean technologies [J]. Environmental Science & Technology, 2012, 46: 3406−3414.

[2] HAQUE N, HUGHES A, LIM S, VERNON C. Rare earth elements: Overview of mining, mineralogy, uses, sustainability and environmental impact [J]. Resources, 2014, 3: 614−635.

[3] GUPTA C, KRISHNAMURTHY N. Extractive metallurgy of rare earths [M]. New York: CRC Press, 2004.

[4] JORDENS A, CHENG Y P, WATERS K E. A review of the beneficiation of rare earth element bearing minerals [J]. Minerals Engineering, 2013, 41: 97−114.

[5] HABASHI F. Extractive metallurgy of rare earths [J]. Canadian Metallurgical Quarterly, 2013, 52: 224−233.

[6] GUPTA C K, KRISHNAMURTHY N. Extractive metallurgy of rare earths [J]. International Materials Reviews, 1992, 37: 197−248.

[7] HABASHI F. The recovery of the lanthanides from phosphate rock [J]. Journal of Chemical Technology and Biotechnology, 2007, 35: 5−14.

[8] ALY M M, MOHAMMED N A. Recovery of lanthanides from Abu Tartur phosphate rock, Egypt [J]. Hydrometallurgy, 1999, 52: 199−206.

[9] KUZMIN V I, PASHKOV G L, LOMAEV V G, VOSKRESENSKAYA E N, KUZMINA V N. Combined approaches for comprehensive processing of rare earth metal ores [J]. Hydrometallurgy, 2012, 129−130: 1−6.

[10] CHAÏRAT C, SCHOTT J, OELKERS E H, LARTIGUE J E, HAROUIYA N. Kinetics and mechanism of natural fluorapatite dissolution at 25 °C and pH from 3 to 12 [J]. Geochimica et Cosmochimica Acta, 2007, 71: 5901−5912.

[11] HAROUIYA N, CHAÏRAT C, KÖHLER S J, GOUT R, OELKERS E H. The dissolution kinetics and apparent solubility of natural apatite in closed reactors at temperatures from 5 to 50 °C and pH from 1 to 6 [J]. Chemical Geology, 2007, 244: 554−568.

[12] AL-OTHMAN A O, SWEILEH J A. Phosphate rock treatment with citric acid for the rapid potentiometric determination of fluoride with ion-selective electrode [J]. Talanta, 2000, 51: 993−999.

[13] OLANIPEKUN E O. Kinetics of dissolution of phosphorite in acid mixtures [J]. Bulletin of the Chemical Society of Ethiopia, 1999, 13: 63−70.

[14] van der SLUIS S, MESZAROS Y, MARCHEE W G J, WESSELINGH H A, van ROSMALEN G M. The digestion of phosphate ore in phosphoric acid [J]. Industrial & Engineering Chemistry Research, 1987, 26: 2501−2505.

[15] BRAHIM K, ANTAR K, KHATTECH I, JEMAL M. Effect of temperature on the attack of fluorapatite by a phosphoric acid solution [J]. Scientific Research and Essay, 2008, 3: 35−39.

[16] ANTAR K, JEMAL M. Kinetics and thermodynamics of the attack of a phosphate ore by acid solutions at different temperatures [J]. Thermochimica Acta, 2008, 474: 32−35.

[17] GUMGUM B. The leaching of yttrium from Avnik (Bingöl-Turkey) apatite by dilute sulfuric acid [J]. Communications, Faculty of Science, University of Ankara, Series B, 1986, 32: 135−140.

[18] KHAWASSEK Y M, ELIWA, A A, GAWAD E A, ABDO S M. Recovery of rare earth elements from El-Sela effluent solutions [J]. Journal of Radiation Research and Applied Sciences, 2015, 8: 583−589.

[19] WANG L, LONG Z, HUANG X, YU Y, CUI D, ZHANG G. Recovery of rare earths from wet-process phosphoric acid [J].

Hydrometallurgy, 2010, 101: 41−47.
[20] KANDIL A T, ALY M M, MOUSSA E M, KAMEL A M, GOUDA M M, KOURAIM M N. Column leaching of lanthanides from Abu Tartur phosphate ore with kinetic study [J]. Journal of Rare Earths, 2010, 28: 576−580.
[21] JORJANI E, BAGHERIEH A H, CHELGANI S C. Rare earth elements leaching from Chadormalu apatite concentrate: Laboratory studies and regression predictions [J]. Korean Journal of Chemical Engineering, 2011, 28: 557−562.
[22] LI H, GUO F, ZHANG Z, LI D, WANG Z. A new hydrometallurgical process for extracting rare earths from apatite using solvent extraction with P350 [J]. Journal of Alloys and Compounds, 2006, 408−412: 995−998.
[23] BEZERRA M A, SANTELLI R E, OLIVEIRA E P, VILLAR L S, ESCALEIRA L A. Response surface methodology (RSM) as a tool for optimization in analytical chemistry [J]. Talanta, 2008, 76: 965−977.
[24] ZHANG Z, PENG J, SRINIVASAKANNAN C, ZHANG Z, ZHANG L, FERNÁNDEZ Y, MENÉNDEZ J A. Leaching zinc from spent catalyst: Process optimization using response surface methodology [J]. Journal of Hazardous Materials, 2010, 176: 1113−1117.
[25] CHEN T, LI B, FANG L, CHEN D, XU W, XIONG C. Response surface methodology for optimizing adsorption performance of gel-type weak acid resin for Eu(III) [J]. Transactions of Nonferrous Metals Society of China, 2015, 25: 4207−4215.
[26] BANDARA A M T S, SENANAYAKE G. Leachability of rare-earth, calcium and minor metal ions from natural fluorapatite in perchloric, hydrochloric, nitric and phosphoric acid solutions: Effect of proton activity and anion participation [J]. Hydrometallurgy, 2015, 153: 179−189.
[27] LIU X, BYRNE R H. Rare earth and yttrium phosphate solubilities in aqueous solution [J]. Geochimica et Cosmochimica Acta, 1997, 61: 1625−1633.
[28] LEVENSPIEL O. Chemical reaction engineering [M]. 3rd ed. New York: John Wiley & Sons, Inc., 1999.
[29] AARABI-KARASGANI M, RASHCHI F, MOSTOUFI N, VAHIDI E. Leaching of vanadium from LD converter slag using sulfuric acid [J]. Hydrometallurgy, 2010, 102: 14−21.

硝酸浸出铁矿废渣磷灰石中铈、镧、钕稀土元素的工艺参数优化及其动力学

A. FERDOWSI, H. YOOZBASHIZADEH

Department of Materials Science and Engineering, Sharif University of Technology, Azadi Ave., Tehran, P. O. Box 11155-9466, Iran

摘　要：采用硝酸浸出铁矿废渣磷灰石中的铈、镧、钕稀土元素，应用响应面方法对硝酸浓度、液固比和浸出时间对稀土元素浸出率的影响进行了研究。结果表明，硝酸浓度和液固比对稀土浸出率的影响较大，而浸出时间的影响较小。在浸出条件为硝酸浓度 18%、液固比 0.06 和浸出时间 38 min 的情况下，可得到最大的铈、镧、钕稀土元素浸出率，其分别为 66.1%、56.8%、517.%。采用收缩核模型对铈的浸出动力学进行研究。结果发现，浸出过程由两个阶段组成，在第一阶段，铈的浸出率随时间增长快速增加；随时间的延长，浸出率增长逐渐变慢。在第一阶段，反应受灰分层内扩散控制，反应的表观活化能为 6.54 kJ/mol；在第二阶段，溶液中的质量传递为反应控制步骤。

关键词：稀土元素；磷灰石；浸出；响应面方法；收缩核模型

(Edited by Sai-qian YUAN)